Contributions towards the prediction of velocity distribution in open channel flows

P.C. Yannopoulos & A.C. Demetracopoulos
Department of Civil Engineering, University of Patras, 265 00 Patras, Greece
Email: acdem@upatras.gr

Abstract

The steady state, depth-averaged hydrodynamic equations are used for the computation of transverse profiles of the longitudinal velocity in prismatic and natural channels. Turbulence closure of the comlete set of equations is accomplished (a) via a simle model in which ν_t is assumed proportional to the shear velocity and the local depth, and (b) the depth-averaged k-ε model of Rastogi & Rodi. Subsequently, the governing equations are simplified to their purely parabolic form and the transverse distance is replaced by the cumulative discharge as the second independent variable. Turbulence closure in the latter set of equations is accomplished with model (a). All models are solved numerically via Patankar's scheme and the results are compared with literature data corresponding to laboratory and field measurements. It is shown that the purely parabolic, transformed-coordinates model is more efficient than, and equally accurate with, the complete model.

1 Introduction

Determination of transverse profiles of the longitudinal velocity in channels and streams has many practical implications. Amongst others, it facilitates computation of stream discharge and is of major importance in mass transport studies where velocity distributions are required for the solution of the advection dispersion equation. In this study we examine channels and streams of large aspect ratio for which the determination of the flow field may be accomplished via the depth-averaged hydrodynamic equations.

2 Equations

2.1 General hydrodynamic equations

The steady state, depth-averaged hydrodynamic equations consist of the continuity equation

$$\frac{\partial(hu)}{\partial x}+\frac{\partial(hv)}{\partial y}=0 \tag{1}$$

and the momentum equations, which can be written as[1]:

$$\frac{\partial(hu\Phi)}{\partial x}+\frac{\partial(hv\Phi)}{\partial y}=\frac{\partial}{\partial x}\left(D_{\Phi x}\frac{\partial\Phi}{\partial x}\right)+\frac{\partial}{\partial y}\left(D_{\Phi y}\frac{\partial\Phi}{\partial y}\right)+S_{\Phi} \tag{2}$$

The x-momentum equation is recovered from eqn (2) for

$$\Phi=u,\quad D_{ux}=0,\quad D_{uy}=h\nu_t,\quad S_u=-gh\frac{dH}{dx}-\frac{\tau_{bx}}{\rho|\cos\theta|} \tag{3}$$

and the y-momentum is recovered from eqn (2) for

$$\Phi=v,\quad D_{vx}=2h\nu_t,\quad D_{vy}=0,\quad S_v=-\frac{1}{\rho}\frac{\partial(hp_d)}{\partial y}-\frac{\tau_{by}}{\rho|\cos\theta|} \tag{4}$$

where h=water depth, H=water surface elevation, τ_{bx}, τ_{by}=bottom shear stresses, p_d= pressure in the transverse direction and θ=transverse angle of inclination at any point of the bottom[2]. The above equations define a flow problem which is parabolic in the longitudinal direction and elliptic in the transverse direction. Bottom shear stresses are given by the relations:

$$\tau_{bi}=\rho c_f u_i\left(u^2+v^2\right)^{1/2},\quad i=x,y\quad\text{and}\quad c_f=\frac{n^2 g}{R^{1/3}} \tag{5}$$

2.2 Turbulence closure

Turbulence closure is achieved with two different models. In the first model, the eddy viscosity, ν_t, is expressed as

$$\nu_t = c_v u_* h \tag{6}$$

in which u_*=shear velocity and c_v=dimensionless eddy viscosity coefficient. A model presented by the authors[3] is used for the transverse variation of c_v. This model assumes a value c_{vm}=0.6 for most of the cross-section and a parabolic variation near the boundaries, leading to a value of zero and slope of κ/h at the banks. Equations (1) through (5) and (6) define the first model, hereafter called XYCV, for determination of the transverse distribution of longitudinal velocities.

The second model for turbulence closure is the depth-averaged k-ε model of Rastogi & Rodi[4]. Therein, ν_t is defined as

$$\nu_t = c_\mu \frac{k^2}{\varepsilon} \tag{7}$$

where k=depth-averaged kinetic energy of turbulent motion and ε=depth-averaged rate of its dissipation. The transport equations of k and ε are recovered from eqn (2) for

$$\Phi = k, \quad D_{kx} = 0, \quad D_{ky} = h\frac{\nu_t}{\sigma_k}, \quad S_k = h\left(G + P_{kv} - \varepsilon\right) \tag{8}$$

$$\Phi = \varepsilon, \quad D_{\varepsilon x} = 0, \quad D_{\varepsilon y} = h\frac{\nu_t}{\sigma_\varepsilon}, \quad S_\varepsilon = h\left(c_1 \varepsilon \frac{G}{k} + P_{\varepsilon v} - c_2 \frac{\varepsilon^2}{k}\right) \tag{9}$$

in which

$$G = \nu_t \left(\frac{\partial u}{\partial y}\right)^2, \quad P_{kv} = c_k \frac{u_*^3}{h}, \quad P_{\varepsilon v} = c_\varepsilon \frac{u_*^4}{h^2} \tag{10a}$$

and

$$c_k = \frac{1}{\sqrt{c_f}}, \quad c_\varepsilon = 3.6\frac{c_2}{c_f^{3/4}}\sqrt{c_\mu} \tag{10b}$$

The constants appearing in the equations take the following values: c_μ=0.09, σ_k=1.0, σ_ε=1.3, c_1=1.43, c_2=1.92 and the von Karman constant is κ=0.42.

Boundary conditions for k and ε are defined at the first internal node which is placed outside of the viscous sublayer. This is achieved by selecting a transverse distance of the first internal node,

y_w, which satisfies the inequality $30<(u_* y_w / \nu)<100$. At that node k and ε are given by[4]:

$$k_w = \frac{u_*^2}{\sqrt{c_\mu}}, \quad \varepsilon_w = \frac{u_*^3}{\kappa y_w} \tag{11}$$

Combination of eqns (1) through (5) and (7) through (11) defines the second model, hereafter called XYKE, for determination of the transverse distribution of longitudinal velocities.

2.3 Fully parabolic transformed-coordinates model

The momentum transport equations resulting from eqns (2), (3) and (4) can be reduced to their purely parabolic form when downstream phenomena do not influence the flow upstream, except for the influence on the longitudinal depth and velocity profiles. In such cases the boundary layer approximations are valid, i.e. $\partial / \partial x << \partial / \partial y$ and $v<<u$. Thus, the purely parabolic form of the hydrodynamic equations reduces to the continuity and the x-momentum equation , i.e. eqns (1) through (3).

In natural streams, where the cross section varies in the longitudinal direction, the problem can be simplified by replacing y with the cumulative discharge, q, measured from one bank

$$q = \int_0^y hud\xi \tag{12}$$

where $0 \le y \le B$ and B=surface width. Transformation of eqns (1) through (3) to a system of (x,q) independent variables yields:

$$\frac{\partial u}{\partial x} = \frac{\partial}{\partial q}\left[\left(\nu_t h^2 u\right)\frac{\partial u}{\partial q}\right] + \frac{g(-dH/dx)}{u} - \frac{\tau_{bx}}{\rho h u^2 |\cos\theta|} u \tag{13}$$

and

$$\frac{\partial q}{\partial y} = uh \quad (a) \quad \text{and} \quad \frac{\partial q}{\partial x} = -vh \quad (b) \tag{14}$$

Note that eqn (13) conforms to the general form of eqn (2), for

$$\Phi \equiv u, \quad h \equiv 1, \quad u \equiv 1, \quad v \equiv 0, \quad y \equiv q, \quad D_{ux} = 0 \tag{15a}$$

$$D_{uy} = \nu_t h^2 u, \quad S_u = \left[\frac{g(-dH/dx)}{u}\right] + \left[-\frac{\tau_{bx}}{\rho h u^2 |\cos\theta|}\right] u \qquad (15b)$$

Turbulence closure is achieved via the model of eqn (6). The resulting model, consisting of eqns (13), (14), (6) and (5), called hereafter XQCV model, is the third model used for determination of the transverse distribution of longitudinal velocities.

3 Numerical solution

The numerical solution of models XYCV and XYKE is based on Patankar's SIMPLER algorithm[5]. Constuction of the staggered control volumes is given in [1]. All hydraulic and geometric parameters take their local values. Solution proceeds in the longitudinal direction until the correct velocity profile is computed. The step Δx is taken equal to the size of the smallest of the large eddies that can be observed in the cross-section. For a composite cross-section of rectangular segments this implies the smallest between half-widths of each rectangle. An under-relaxation coefficient of 0.8 is used at each successive step.

The numerical solution of the XQCV model does not require the use of the SIMPLER algorithm because the pressure term is not present. It does require, however, the use of a successive iterations technique since the diffusion coefficient and the coefficients of the source term are functions of the unknown velocity u. In the manner of the previous two models, the numerical solution can be viewed as one commencing from an initial estimate of the transverse distribution of u, and marching in the longitudinal direction until convergence to the true solution is attained.

Determination of nodes on the q-axis, is based on the velocity distribution at the previous step, u_i^p, and is given by the relations

$$q_{e_i}^p = q_{e_{i-1}}^p + u_i^p h_i \left(y_{e_i} - y_{e_{i-1}}\right) \quad \text{with} \quad q_{e_o}^p = 0 \qquad (16a)$$

$$q_i^p = \frac{1}{2}\left(q_{e_{i-1}}^p - q_{e_i}^p\right) \qquad (16b)$$

where the subscript e indicates control volume interface. It is assumed that the values of u_i at the next step correspond to nodes y_i and are used for the computation of new cumulative discharge

values, q_i. Convergence is based on the continuity equation and is formulated as follows:
(a) Eqn (14b) is utilized for the computation of transverse velocities

$$v_{e_i} = -\frac{1}{h_i}\left(\frac{q_{e_i} - q_{e_i}^p}{\Delta x}\right) \tag{17}$$

(b) Satisfaction of the continuity equation is checked as a source term

$$MS_i = h_i\left[\left(u_i - u_i^p\right)\Delta y_i + \left(v_{e_i} - v_{e_{i-1}}\right)\Delta x\right] \tag{18}$$

(c) Since $MS_i \neq 0$ during the initial steps, the cumulative absolute volume source is formulated as

$$CAMS = \sum_{i=1}^{N} |MS_i| \tag{19}$$

where N=number of nodes. This quantity is compared with the total volume flux, Q, which is computed from the latest velocity distribution. Convergence is attained when $CAMS \leq 10^{-5} Q$.

4 Results and discussion

The models presented herein were compared with laboratory data collected in two different flumes with trapezoidal and rectangular, respectively, composit cross-sections[6]. The trapezoidal flume was hydraulically smooth with bottom slope 1.027×10^{-3}, while the rectangular one was smooth in the main channel and rough in the flood plain with bottom slope 9.93×10^{-4}.

Observation of velocity distributions in composite cross-sections shows that the difference between maximum velocity in the main channel and the flood plain increases with increasing depth. This causes a stronger transverse exchange of momentum, which in turn controls longitudinal velocities in the main channel. Thus, main channel velocities are strongly affected by roughness characteristics and flow depth in the flood plain. The experimental data in [6] show that for small flood plain depths, total discharge is essentially equal with the discarge of the main channel flowing full. Numerical

experiments showed that separate roughness coefficients must be used for ratios of flood plain to main channel depth smaller than 0.2, and a weighted-average value for ratios larger than 0.2. This is done by equating the total motion-resisting force to the sum of such forces in each segment.

Comparison of the three models with the experimental data for the trapezoidal cross-section, corresponding to main channel flow depth of 0.178 m, are shown in Figure 1. Comparisons for the stage-discharge curves are given in Figure 2. Finally, comparisons with data from a river cross-section[7] are shown in Figure 3.

All three models perform satisfactorily with better performance provided by the XQCV and XYCV models. This indicates that for depth-averaged solutions, the simpler model of eqn (6) may be more appropriate and that the (x,q) formulation is preferable because it is easier to program and implement.

References

[1] Yannopoulos, P.C. & Demetracopoulos, A.C., Computation of flow and mass transport in channels with composite cross section, *Proc. Water Pollution II: Modelling, Measuring and Prediction*, eds. L.C. Wrobel & C.A. Brebbia, Comp. Mech. Publ., Southampton, pp. 151-158, 1993.

[2] Keller, R.J. & Rodi, W. Prediction of flow characteristics in main channel/flood plain flows, *J. Hydraulic Res. (IAHR)*, **26(4)**, pp. 425-441, 1988.

[3] Yannopoulos, P.C. & Demetracopoulos, A.C., A unified approach for the computation of velocity distributions in streams, *Proc. Intl. Conf. Restoration and Protection of the Environment II*, eds. A.C. Demetracopoulos, C.D. Hadjitheodorou & G.P. Korfiatis, University of Patras Press, Patras, pp. 49-56, 1994.

[4] Rastogi, A.K. & Rodi, W. Predictions of heat and mass transfer in open channels, *J. Hydraulics Div. (ASCE)*, **104(HY3)**, pp. 397-420, 1978.

[5] Patankar, S.V., *Numerical Heat Transfer and Fluid Flow*, McGraw-Hill, New York, 1980.

[6] Lambert, M.F. & Sellin, R.H.J. Discharge prediction in straight compound channels using the mixing length concept, *J. Hydraulic Res. (IAHR)*, **34(3)**, pp. 381-394, 1996.

[7] Ackers, P. Hydraulic design of two-stage channels, *Proc. Instn. Civ. Engrs Wat., Marit. & Energy*, **96**, pp. 247-257, 1992.

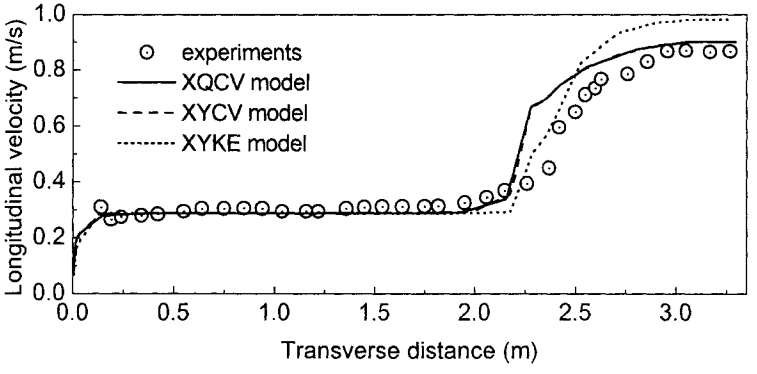

Figure 1: Transverse distribution of longitudinal velocities

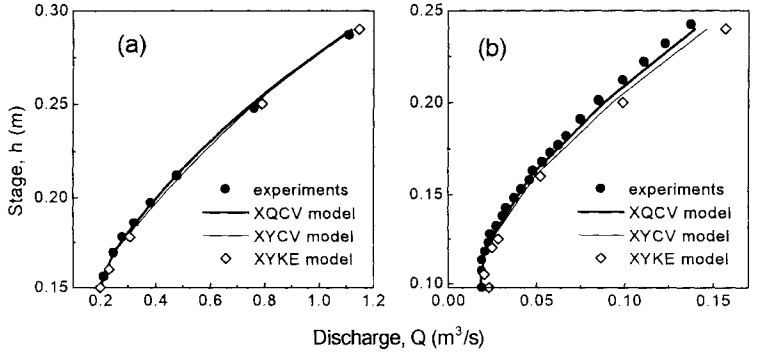

Figure 2: Stage-discharge curves for data of [6]. (a) trapezoidal and (b) rectangular composite cross-sections

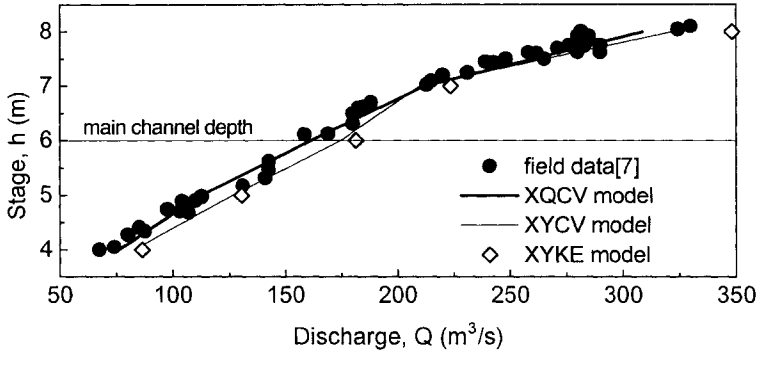

Figure 3: Stage-discharge curve for a riverine cross-section